MOLECULAR AND CELLULAR BIOLOGY, Oct. 2003, p. 6780–6789 Vol. 23, No. 19
0270-7306/03/$08.00+0 DOI: 10.1128/MCB.23.19.6780–6789.2003

Targeted Disruption of the Mouse PAS Domain Serine/Threonine Kinase PASKIN

Dörthe M. Katschinski,[1] Hugo H. Marti,[2] Klaus F. Wagner,[3,4] Junpei Shibata,[3,4] Katrin Eckhardt,[5] Falk Martin,[5] Reinhard Depping,[3] Uwe Paasch,[6] Max Gassmann,[7] Birgit Ledermann,[8] Isabelle Desbaillets,[7]† and Roland H. Wenger[5]*

Cell Physiology Group, Medical Faculty, Martin Luther University Halle, D-06112 Halle,[1] Institute of Physiology[3] and Clinic of Anaesthesiology,[4] University of Lübeck, D-23538 Lübeck, and Carl Ludwig Institute of Physiology[5] and Clinic of Dermatology,[6] University of Leipzig, D-04103 Leipzig, Germany, and Institutes of Physiology,[2] Veterinary Physiology,[7] and Laboratory Animal Science,[8] University of Zürich, CH-8057 Zürich, Switzerland

Received 31 March 2003/Returned for modification 28 May 2003/Accepted 30 June 2003

PASKIN is a novel mammalian serine/threonine kinase containing two PAS (Per-Arnt-Sim) domains. PASKIN is related to the *Rhizobium* oxygen sensor protein FixL and to AMP-regulated kinases. Like FixL, the sensory PAS domain of PASKIN controls the kinase activity by autophosphorylation in a (unknown) ligand-dependent manner. In *Saccharomyces cerevisiae*, the two PASKIN orthologues PSK1 and PSK2 phosphorylate three translation factors and two enzymes involved in glycogen synthesis, thereby coordinately regulating protein synthesis and glycolytic flux. To elucidate the function of mammalian PASKIN, we inactivated the mouse *Paskin* gene by homologous recombination in embryonic stem cells. *Paskin*$^{-/-}$ mice showed normal development, growth, and reproduction. The targeted integration of a *lacZ* reporter gene allowed the identification of the cell types expressing mouse PASKIN. Surprisingly, PASKIN expression is strongly upregulated in postmeiotic germ cells during spermatogenesis. However, fertility and sperm production and motility were not affected by the PASKIN knockout. The *Ppp1r7* gene encoding Sds22, a regulatory subunit of protein phosphatase 1, shares the promoter region with the *Paskin* gene, pointing towards a common transcriptional regulation. Indeed, Sds22 colocalized with the cell types expressing PASKIN in vivo, suggesting a functional role of protein phosphatase-1 in the regulation of PASKIN autophosphorylation.

The PAS (Per-Arnt-Sim) domain is a widespread protein fold of environmental protein sensors involved in the perception of light intensity, oxygen partial pressure, redox potentials, and voltage (9, 18, 26, 29). While most PAS proteins are known from the archaea, bacteria, and lower eukarya, relatively few sensor PAS proteins have been reported in mammalian species. Apart from the HERG voltage-dependent potassium channel (15), the mammalian PAS domain-containing proteins identified so far serve as heterodimerization interfaces of transcription factors involved in the xenobiotic response (25), adaptation to hypoxia (28), circadian rhythm generation (19), and possibly, carbon monoxide signaling (7).

By database searches with the PAS sequence as a bait, we and others previously identified a novel mammalian PAS protein, termed PASKIN (10) or PAS kinase (22). The domain architecture of PASKIN resembles that of the oxygen sensor protein FixL from *Rhizobium* species which contains a heme-bearing PAS domain and a histidine kinase domain that couples sensing to signaling (8). PASKIN contains two PAS domains, with higher sequence similarity to the FixL PAS domain than to any other known PAS domain, and a serine/threonine kinase domain related to AMP kinases. As known from FixL, the PAS A domain of PASKIN represses the kinase activity in *cis*. Following derepression, presumably by ligand-binding to the PAS domain, autophosphorylation in *trans* results in the switching on of the kinase domain of PASKIN (22).

Of note, the human *PASKIN* and mouse *Paskin* genes share a relatively small promoter region with *PPP1R7* and *Ppp1r7*, respectively, suggesting coexpression of the two genes (10). *PPP1R7*/*Ppp1r7* encodes for Sds22, the regulatory subunit 7 involved in target protein recognition of the serine/threonine protein phosphatase 1 (PP1) (2–4). Thus, it is tempting to speculate that Sds22 directs PP1-mediated dephosphorylation of activated PASKIN, resulting in the switching off of the PASKIN kinase activity.

The three-dimensional structure of the PASKIN PAS A domain has recently been resolved, and synthetic ligands binding to this domain were identified (1). Ligand binding as well as mutation of the PAS A domain result in the activation of the kinase domain. The synthetic ligands identified are structurally related to dioxin, known to bind to the PAS domain of the dioxin receptor. However, an endogenous ligand of PASKIN has not been identified so far. While the physiological function of mammalian PASKIN is unknown, important insights into the function of the two *Saccharomyces cerevisiae* homologs have recently been obtained (23). The yeast PASKIN homologs phosphorylate three translation factors and two enzymes involved in the regulation of glycogen and trehalose synthesis, thereby coordinately controlling translation and

* Corresponding author. Mailing address: Carl Ludwig Institute of Physiology, University of Leipzig, Liebigstrasse 27, D-04103 Leipzig, Germany. Phone: 49 0 341 97 15567. Fax: 49 0 341 97 15509. E-mail: wenr@medizin.uni-leipzig.de.

† Present address: Laboratory of Tumor Biology and Genetics, Centre Hospitalier Universitaire Vaudois, CH-1011 Lausanne, Switzerland.

sugar flux. Under stress conditions (nutrient restriction combined with high temperature), PASKIN kinase activity results in downregulation of protein synthesis and carbohydrate storage (23).

Overall, the data on PASKIN function obtained so far are consistent with its role as a putative sensory protein: the PAS domain measures the concentration of a (possibly metabolic) ligand, a PAS domain-triggered interplay between autophosphorylation and phosphatase activities controls the activation switch of an intrinsic serine/threonine kinase, and this kinase finally signals the information to critical factors of the translational and metabolic machineries. Moreover, as might be expected for a sensory protein, PASKIN is ubiquitously expressed at rather low levels (10). In order to understand the physiological role of PASKIN in mammals, we targeted the mouse *Paskin* gene by homologous recombination. Surprisingly, very high PASKIN expression levels were detected in the testis during spermatogenesis.

MATERIALS AND METHODS

Generation of mutant mice. An *Xho*I fragment of the 129Sv(ev) genomic λ phage clone λP1, containing mouse *Paskin* exons 7 to 15, was subcloned into pBluescript KSPII (Stratagene), yielding the plasmid pP1X (10). pP1X was cleaved with *Sal*I to remove exons 10 to 14, and a *Sal*I fragment derived from pGT1.8Iresβgeo (kind gift of A. Smith, Edinburgh, United Kingdom) was inserted instead, resulting in the targeting vector pPKO. To remove bacterial sequences, pPKO was cleaved with *Xho*I and the insert was purified by agarose gel electrophoresis and electroelution. The targeting vector was electroporated into TC-1 embryonic stem (ES) cells derived from 129Sv mice (6). Following selection with 250 μg of G418 (Calbiochem, La Jolla, Calif.)/ml, resistant ES clones were analyzed by Southern blotting. ES clones containing a homologously recombined *Paskin* allele were transferred into (C57BL/6 × DBA/2)F_1 blastocysts which were reimplanted into NMRI foster mice. Chimeric male mice were crossed with C57BL/6 female mice, and germ line transmission was analyzed by PCR. Heterozygous offspring were bred to homozygosity. All experimental protocols were performed following the Swiss Animal Protection Law and were supervised by the Veterinary Department of the Kanton Zürich.

DNA analysis. Genomic DNA was isolated from ES cell cultures and tail biopsy specimens by using standard techniques (24). Southern blotting was performed as described previously (10). Briefly, genomic DNA was digested with *Ecl*136II and the Southern blots were hybridized to a radioactively labeled 582-bp *Xho*I-*Ecl*136II fragment derived from the overlapping phage clone λP5 (10). PCR analysis was performed with 100 ng of mouse tail genomic DNA with the primers PKO5.1 (5′-TTTGTCAGGGTTTGGGGTAG-3′), PKO3.1 (5′-GCACAAAAGCACCGTGTCTA-3′), and En3.1 (5′-TGTCCTCCAGTCTCCTCCAC-3′) simultaneously. PCR conditions were 35 cycles of 94°C for 30 s, 60°C for 30 s, and 72°C for 90 s.

RNA analysis. Mice were sacrificed by cervical dislocation, and the organs were excised and rapidly frozen in liquid nitrogen. These experimental protocols were performed according to the German Animal Protection Law (Ministry for Nature and Environment of Schleswig-Holstein application number 21/A21/02). Total RNA isolation and analysis by Northern blotting was performed as described previously (20). Hybridization probes spanning the PAS or kinase domains of PASKIN were isolated from the mouse PASKIN cDNA 3′ end (clone IMAGp998H022323) and the human PASKIN cDNA 5′ end (clone HA0/203), respectively, as described before (10). The β-*geo* probe was isolated from the plasmid pGT1.8Iresβgeo. The ribosomal protein L28 cDNA probe was described before (20), and the Sds22 cDNA was a kind gift of M. Bollen (Leuven, Belgium).

X-Gal staining. For whole-mount 5-bromo-4-chloro-3-indolyl-β-D-galactopyranoside (X-Gal) staining, excised mouse organs were fixed in 0.2% glutaraldehyde, 5 mM EGTA, 2 mM $MgCl_2$, and 0.1 M Na-phosphate buffer (pH 7.3); permeabilized in 0.01% Na-deoxycholate, 0.02% NP-40, 2 mM $MgCl_2$, and 0.1 M Na-phosphate buffer (pH 7.3); and incubated in X-Gal solution [5 mM $K_3Fe(CN)_6$, 5 mM $K_4Fe(CN)_6$, 2 mM $MgCl_2$, 0.02% NP-40, 0.01% Na-deoxycholate, 0.1 M Na-phosphate buffer (pH 7.3), 0.1% X-Gal] for 1 h at 30°C. For cryosection analysis, excised mouse organs were washed in phosphate-buffered saline (PBS) at 4°C and fixed for 4 h at 4°C in 1% formaldehyde, 5 mM EGTA, and 2 mM $MgCl_2$. Following incubation in 18% sucrose overnight, the organs were embedded in Tissue Tek and frozen in dry ice-isopentane. Cryosectioned 5-μm-thick slices were dried, fixed as described above for 3 min, washed with PBS, and incubated in X-Gal solution overnight at 30°C. The sections were washed in PBS, counterstained with neutral red, fixed with ethanol, and mounted in Entelan.

In situ hybridization. In situ hybridization was performed as described previously (13). The mouse PASKIN hybridization probe was obtained by subcloning a 510-bp *Eco*RI-*Nhe*I fragment derived from the plasmid p934321 (10) into the *Eco*RI-*Xba*I sites of pBluescript SKII (Stratagene). Single-stranded antisense or sense cRNA probes were generated by in vitro transcription of these plasmids with 100 μCi of ^{35}S-UTP and T7 or T3 RNA polymerases. Adult male C57BL/6 mice from an in-house breeding facility were killed by decapitation, and both testes were removed, embedded in Tissue Tek O.C.T. (Miles Scientific), and transferred into a mixture of methyl butane and dry ice until frozen. The blocks were stored at −70°C. Sections (10 μm thick) were cut with a cryostat and melted on silane-coated glass slides. Sections were incubated in 2× SSC (1× SSC is 0.15 M NaCl plus 0.015 M sodium citrate) at 70°C, digested with Pronase (40 μg/ml), fixed in 4% paraformaldehyde, and acetylated with acetic anhydride diluted 1:400 in 0.1 M triethanolamine. Hybridization was performed in buffer containing 50% formamide, 10% dextran sulfate, 10 mM Tris-HCl (pH 7.5), 10 mM sodium phosphate (pH 6.8), 2× SSC, 5 mM EDTA, 150 μg of yeast tRNA/ml, 0.1 mM UTP, 1 mM β-S-ADP, 1 mM γ-S-ATP, 10 mM dithiothreitol, 10 mM 2-mercaptoethanol, and 3×10^4 cpm of ^{35}S-labeled RNA probe/ml overnight at 48°C. Slides were washed in 2× SSC–50% formamide at 42°C for 4 h, digested with RNase (20 μg/ml) for 30 min, washed again with 2× SSC–50% formamide overnight, and dehydrated in graded ethanol. Slides were coated with Kodak NTB-2 emulsion (Eastman Kodak, Rochester, N.Y.) diluted 1:1 in water and exposed for 29 days. Slides were developed and counterstained with 0.02% toluidine blue, air dried, and mounted.

Sperm analysis. Mice were sacrificed by cervical dislocation, and testes, capita epididymides, caudal epididymides, and vasa deferentia were isolated and weighed on a precision balance. Tissues were minced with a scalpel into 1 ml of prewarmed (37°C) BWW medium (4.78 mM KCl, 1.71 mM $CaCl_2$, 1.19 mM $MgSO_4$, 1.19 mM KH_2PO_4, 25.07 mM $NaHCO_3$, 94.7 mM NaCl, 20 mM HEPES [pH 7.4], 21.58 mM lactate, 0.5 mM pyruvate, 20 U of penicillin/ml, 20 μg of streptomycin/ml, 5.56 mM glucose, 5 mg of bovine serum albumin/ml) in six-well cell culture dishes. After 15 min at 37°C, sperm cell suspensions were carefully pipetted from the supernatant and filtered through 40-μm-pore-size nylon mesh (cell strainer; Falcon), and viability was assessed by eosin staining. Following fixation with 1.85% formaldehyde in PBS, sperm counts were estimated by using a Beckmann Coulter Z2 particle count and size analyzer with a particle size selection of 3 to 8 μm. Motility was analyzed by computer-assisted sperm motility analysis (CASA) with a cell motion analyzer (Mika Medical GmbH, Montreux, Switzerland). Aliquots (5 μl) of sperm suspensions were placed into disposable counting chambers (thickness = 10 μm) on a 37°C microscope stage warmer. A minimum of 200 spermatozoa were analyzed from each specimen with the following parameters: number of frames, 32; minimum area of sperm head, 10 pixels; maximum area, 100 pixels; immotile cell velocity curve linear (VCL), <5 μm/s; nonprogressive motile cell VCL, <10 μm/s; tail detection, 5 pixels; and tail size, 15 pixels. The correct identification of sperm cells was given by the tail detection system. Of the determined parameters, the VCL (in micrometers/second), velocity average path (VAP) (in micrometers/second), and velocity straight line (VSL) (in micrometers/second) of the motile population were considered in our experiments.

Protein analysis. Protein extract preparation from mouse organs and immunoblot analysis were performed as described before (12). Rabbit polyclonal antibodies derived against N- and C-terminal peptides of Sds22 were kindly provided by M. Beullens and M. Bollen. A mouse monoclonal anti-β-actin antibody was purchased from Sigma. Immunohistochemistry of mouse testis was performed as described previously (13).

RESULTS

Targeted disruption of *Paskin* in mice. A targeting vector was constructed to replace exons 10 to 14 of the mouse *Paskin* gene by homologous recombination (Fig. 1A). The promoterless expression cassette contained an En-2 splice acceptor site, an internal ribosome entry site, and β-*geo*, a fusion between the *lacZ* and *neo* genes (16). Previous Northern blot analysis revealed PASKIN mRNA expression in various ES cell lines

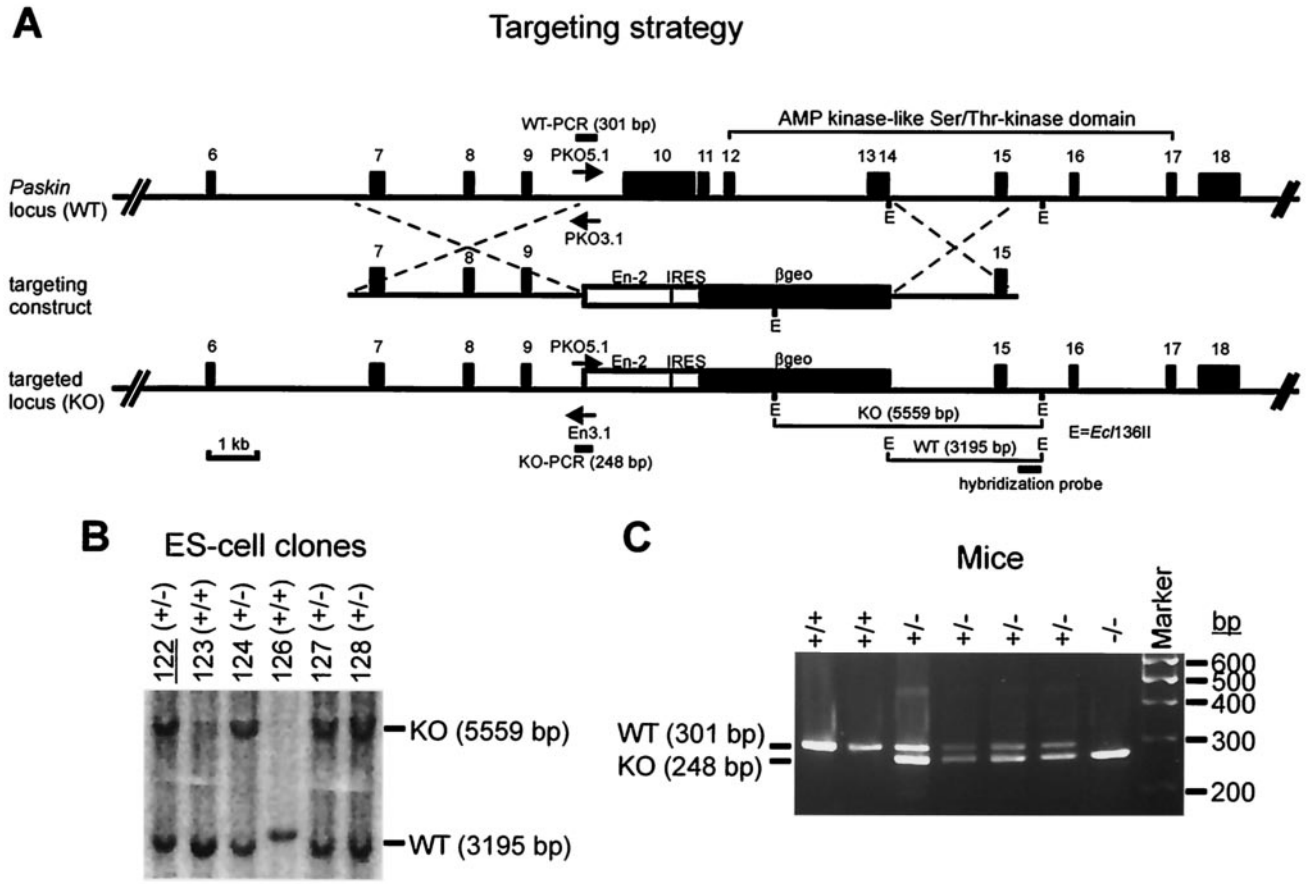

FIG. 1. Generation of mice containing a mutant *Paskin* gene. (A) Targeting and genotyping strategies. The promoterless targeting vector contained a splice acceptor (En-2), an internal ribosome entry site, and a fusion of the *neo* and *lacZ* genes (β-*geo*). Southern and PCR genotyping strategies at the 3′ and 5′ ends of the targeting vector, respectively, are indicated. E, *Ecl*136II. (B) Southern blot analysis of G418-resistant ES cell clones. ES clone no. 122 was used to generate *Paskin* knockout mice. (C) PCR analysis of genomic DNA obtained from mouse tail biopsies. The three primers shown in panel A were used in each PCR simultaneously. The lengths of the wild-type (WT) and knockout (KO) alleles are indicated.

(data not shown). Therefore, expression of the β-*geo* gene following homologous recombination in transfected ES cells is driven by the endogenous *Paskin* promoter. Southern blotting of the G418-resistant ES cell colonies (Fig. 1B) revealed a homologous recombination efficiency of 30%. The ES clone 122 was used for the generation of chimeric *Paskin* knockout mice. Germ line transmission of the targeted *Paskin* allele was determined by PCR analysis of genomic DNA isolated from tail biopsies (Fig. 1C). Heterozygous mice ($Paskin^{+/-}$) were intercrossed to obtain homozygous mutant mice ($Paskin^{-/-}$).

Normal fertility and development of *Paskin* knockout mice. Offspring of *Paskin* wild-type, heterozygous, and knockout intercrossings displayed normal litter sizes, suggesting normal fertility and embryonic development (Table 1). Mendelian frequencies of the transmitted genotypes with normal distribution of male and female mice were obtained (data not shown). Both male and female $Paskin^{-/-}$ mice showed normal growth (i.e., gain in body weight), no gross morphological or behavioral alterations, and at least up to the age of 14 months, no difference in viability (data not shown). Organ histology did not reveal any differences between wild-type and knockout mice (data not shown). Thus, these results suggest the absence of obvious detrimental effects of PASKIN deficiency on development, growth, and reproduction.

PASKIN mRNA is highly expressed in the testis. To confirm efficient gene targeting, Northern blot analysis of mouse organs was performed (Fig. 2). PASKIN mRNA expression is generally very low in most mouse tissues. In contrast, a previously unrecognized strong signal was obtained with testis RNA. PASKIN mRNA expression in testis was 90-fold higher than in thymus, the organ with the second highest PASKIN mRNA levels observed (Fig. 2). When Northern blots were probed with a cDNA fragment derived from the targeted ki-

TABLE 1. Litter size of *Paskin* wild-type and knockout mice

Breeding pair (male × female)	Litter size (mean ± SD)	Total no. of offspring
$Paskin^{+/-} \times Paskin^{+/+}$[a]	6.40 ± 3.36	32
$Paskin^{+/-} \times Paskin^{+/-}$	6.97 ± 2.74	446
$Paskin^{-/-} \times Paskin^{+/-}$	8.57 ± 2.37	60
$Paskin^{-/-} \times Paskin^{-/-}$	7.75 ± 3.41	93

[a] C57BL/6.

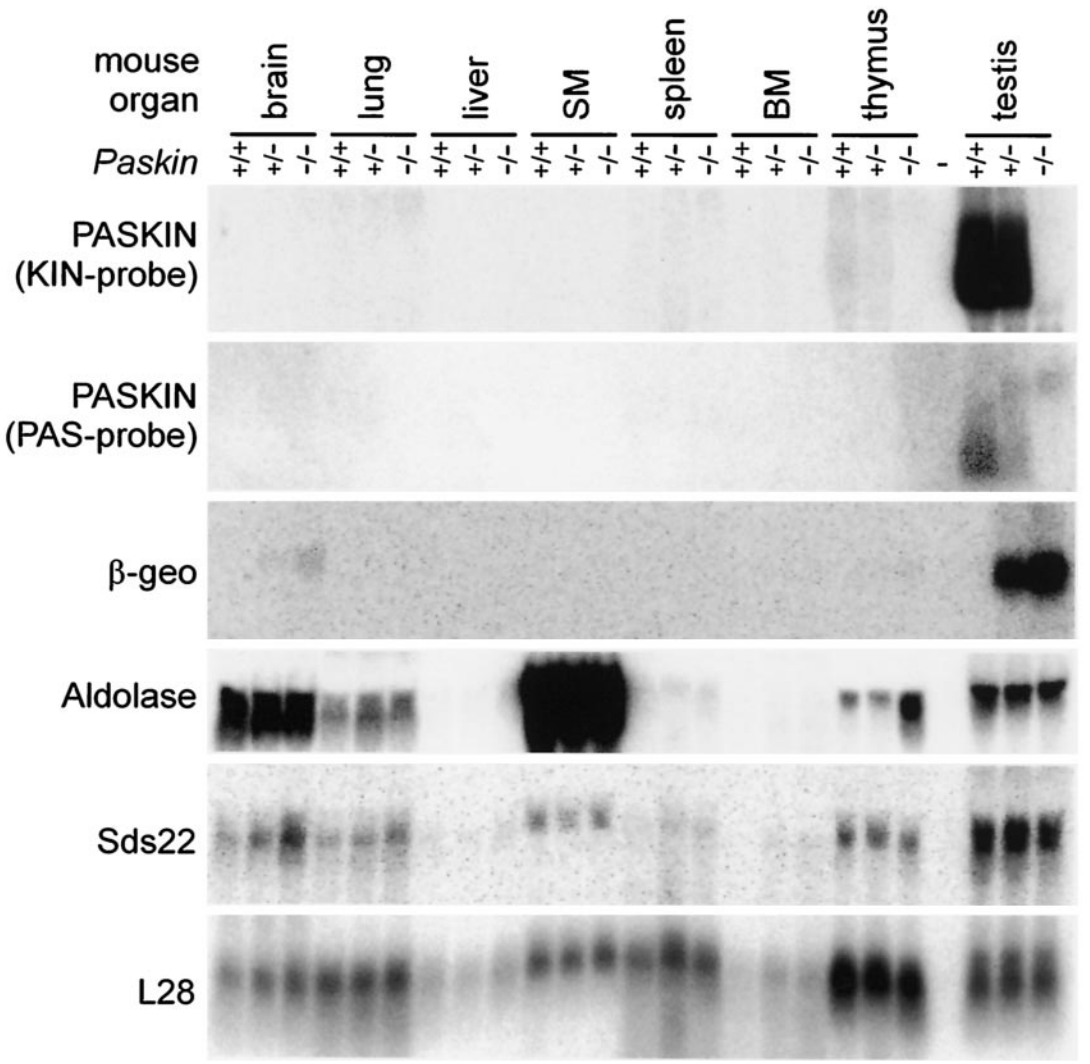

FIG. 2. Expression of PASKIN mRNA in mouse testis. Northern blot analysis of total RNA isolated from the indicated tissues derived from wild-type (*Paskin*$^{+/+}$), heterozygous (*Paskin*$^{+/-}$) and knockout (*Paskin*$^{-/-}$) mice. The blot was subsequently hybridized to the indicated probes. The signal obtained with the cDNA probe encoding the ribosomal protein L28 served as a control for equal loading and blotting efficiency. Note that the 5′ PAS probe was derived from the human PASKIN cDNA and, hence, resulted in a weaker signal with mouse tissue mRNA than the 3′ KIN probe derived from mouse PASKIN.

nase domain (Fig. 1A), PASKIN mRNA levels were reduced by 50% in the testes of *Paskin*$^{+/-}$ mice and were undetectable in *Paskin*$^{-/-}$ mice, confirming the targeted inactivation of the *Paskin* gene (Fig. 2). When a hybridization probe derived from the PAS domain upstream of the targeting site was used, a novel higher-molecular-weight mRNA signal of the targeted *Paskin* mutant allele appeared, replacing the mRNA signal of the wild-type *Paskin*$^{+}$ allele (Fig. 2). This band coincided with the signal obtained with a β-*geo* cDNA probe derived from the targeting vector which was exclusively detectable with the targeted *Paskin* mutant allele but not with the wild-type *Paskin*$^{+}$ allele. These results demonstrate efficient expression of the β-*geo* reporter gene under the control of the *Paskin* promoter and suggest that reporter gene activity can be used to analyze PASKIN expression in the testis. Since the PASKIN orthologues in yeast are involved in glucose flux, we analyzed the expression of a glycolytic enzyme in the targeted mouse strains. As shown in Fig. 2, aldolase mRNA levels did not change in most of the organs analyzed, except in the thymus, where aldolase mRNA was increased in *Paskin*$^{-/-}$ mice.

PASKIN expression is upregulated during spermatogenesis. In order to identify the cell type(s) expressing PASKIN in mouse testis, whole-mount X-Gal staining for β-galactosidase reporter gene activity was performed (Fig. 3A). No other tissue, including ovary and uterus, revealed any blue-staining cells (data not shown), confirming that the testis is the main PASKIN-expressing organ. Blue color developed in distinct regions of the seminiferous tubules in *Paskin*$^{+/-}$ mouse testes, which was stronger in *Paskin*$^{-/-}$ littermates and absent in *Paskin*$^{+/+}$ littermates (Fig. 3A). Nonequal staining within different regions of the seminiferous tubules suggested PASKIN expression in germ cells during spermatogenesis, which occurs in synchronized waves of distinct developmental steps (21). Indeed, mouse testis sections revealed β-galactosidase re-

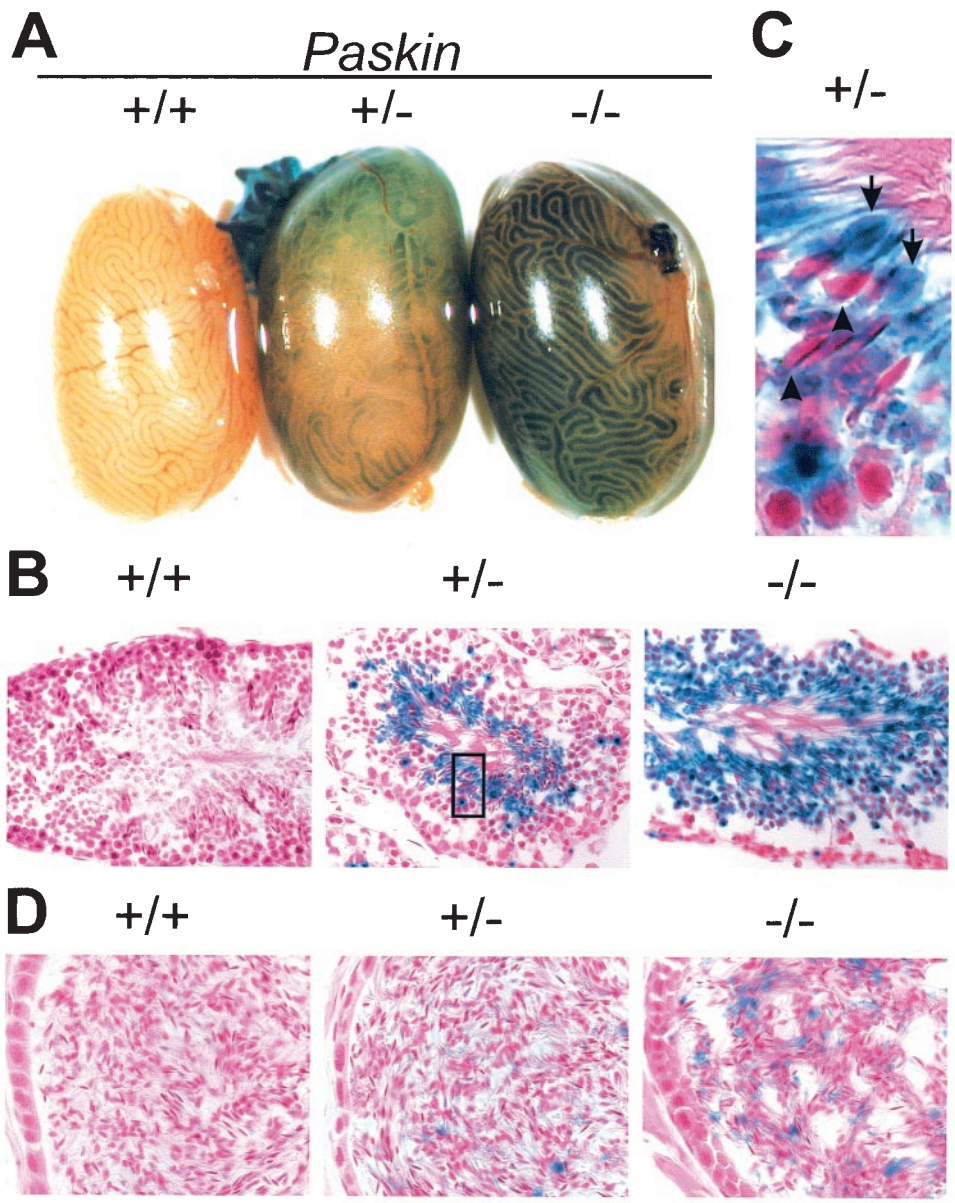

FIG. 3. Germ cell-specific *lacZ* reporter gene activity in male *Paskin*$^{+/-}$ and *Paskin*$^{-/-}$ mice. β-Galactosidase activity in *Paskin* knockout mice detected by X-Gal staining of whole-mount testes (A), testis cryosections (B and C) and epididymides cryosections (D). (C) Arrows denote blue cytoplasmic bulges in the tail of maturating spermatozoae and the arrowheads depict counterstained red spermatozoal heads. The section magnified in panel C is indicated by a rectangle in panel B. Original magnification, ×400 (B) and ×630 (D).

porter gene activity in the luminal regions overlapping with the cytoplasm of round and elongated spermatids (Fig. 3B). While approximately 50% of the round spermatids stained blue in *Paskin*$^{+/-}$ mice, all spermatids were β-galactosidase positive in *Paskin*$^{-/-}$ littermates, further demonstrating that PASKIN expression is confined to haploid germ cells which contain either the *Paskin*$^{+}$ or the *Paskin* mutant allele only.

High-magnification pictures showed the presence of β-galactosidase in bulges of the tail region of maturing spermatozoa which correspond to residual bodies containing most of the remaining cytoplasm (Fig. 3C). Residual bodies transported for degradation to the basal regions of the seminiferous tubules might explain the occasional presence of single blue-staining spots within this region (Fig. 3B). β-Galactosidase leftovers in cytoplasmic droplets might also explain the faint blue staining in spermatozoa stored in the epididymides of *Paskin*$^{-/-}$ mice (Fig. 3D). Some rare blue-staining cells in the epididymides probably correspond to spermatids.

To directly analyze PASKIN mRNA expression in wild-type mouse testis, in situ hybridization was performed. As observed by silver grain visualization in the dark field, PASKIN antisense but not sense probes revealed a distinct expression pattern in different regions of the seminiferous tubules (Fig. 4A). At a higher magnification, silver grains overlapped with spermatocytes, spermatids, and spermatozoa but not with spermatogonia or Leydig cells (Fig. 4B). To determine more precise-

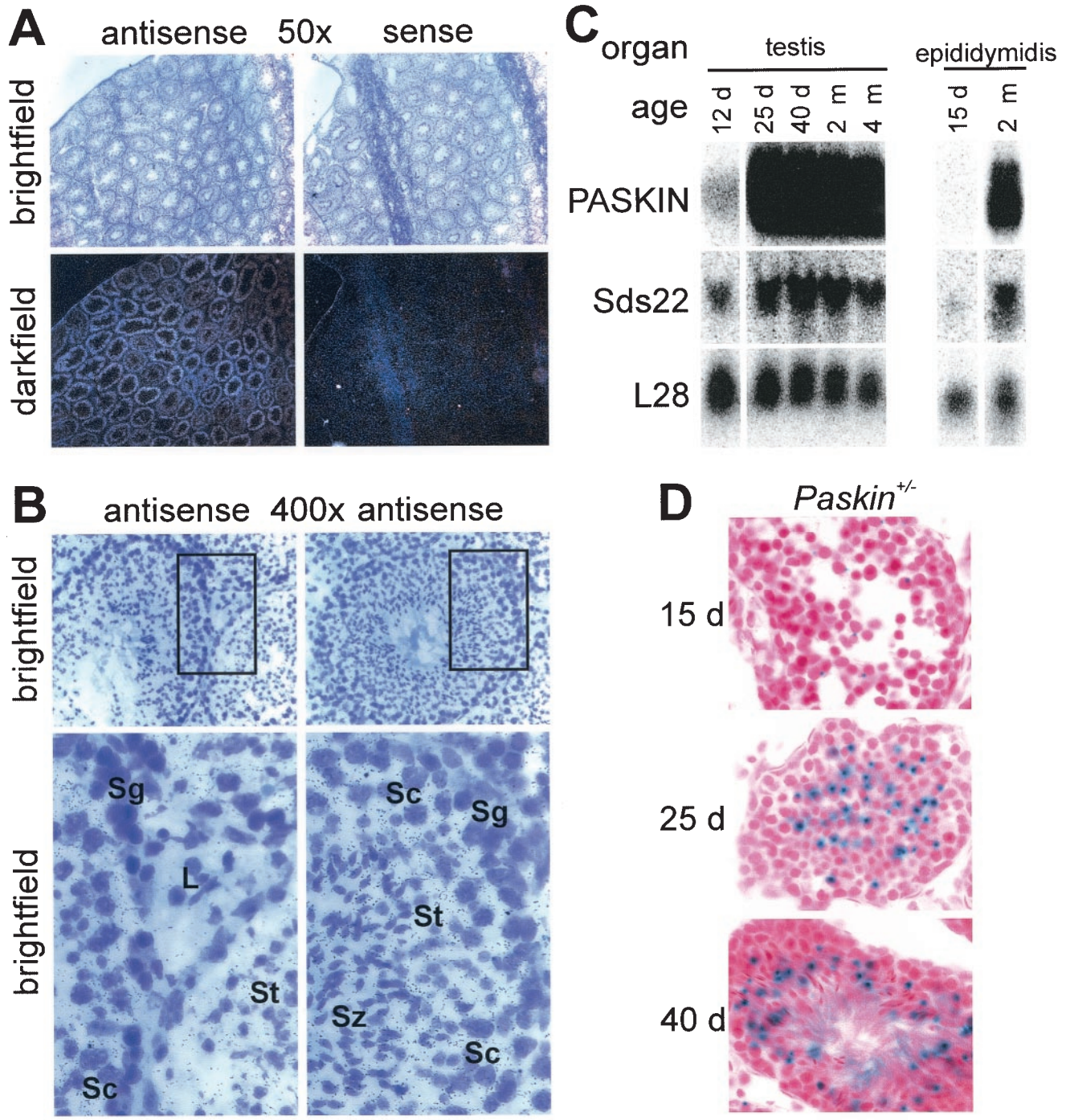

FIG. 4. PASKIN expression in male adult und juvenile mice. (A) In situ hybridization analysis of PASKIN mRNA expression in testis of adult wild-type mice with PASKIN antisense and sense (control) cRNA probes as indicated. Original magnification, ×50 (A) and ×400 (B). The sections magnified in the bottom part of panel B are indicated by rectangles in the upper part of the panel. L, Leydig cells; Sg, spermatogonia; Sc, spermatocytes; St, spermatids; Sz, spermatozoa. (C) Northern blot analysis of total RNA isolated from testes and epididymides of juvenile and adult wild-type mice. All data were derived from one single blot sequentially hybridized with the indicated probes as described for Fig. 2. (D) X-Gal staining of testis cryosections derived from juvenile *Paskin*$^{+/-}$ mice of the indicated ages. d, days; m, months.

ly the developmental state of the onset of PASKIN expression in spermatogenesis, juvenile male mice were analyzed during puberty. On the mRNA level (Fig. 4C) as well as on the level of β-galactosidase reporter gene activity (Fig. 4D), PASKIN expression was almost absent in testis at postnatal day 12 to 15. However, at postnatal day 25, a strong increase in PASKIN mRNA levels (Fig. 4C) as well as in β-galactosidase expression (Fig. 4D) could be observed. PASKIN expression persisted at day 40 (Fig. 4C and D), when spermatozoa could be observed (Fig. 4D), as well as in adult (2 and 4 months) mice (Fig. 4C).

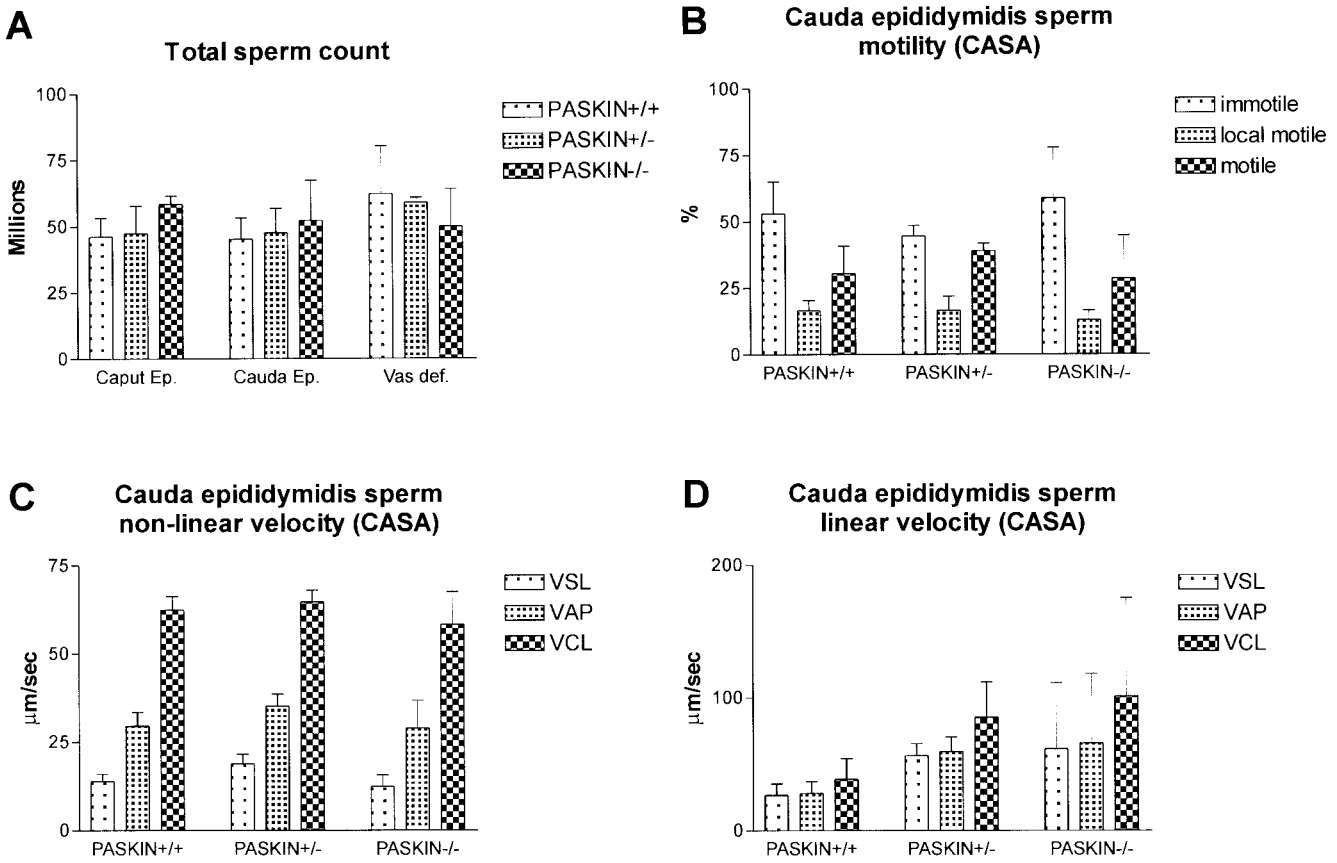

FIG. 5. Functional analysis of sperm cells derived from wild-type *Paskin*$^{+/+}$, heterozygous *Paskin*$^{+/-}$, and knockout *Paskin*$^{-/-}$ mice. (A) Total counts of sperm cells isolated from caput epididymides, caudal epididymides, and vasa deferentia. (B to D) CASA of motility (B) and velocity of nonlinearly (C) and linearly (D) motile sperm cells isolated from caudal epididymides. The VCL, VAP, and VSL are measured. (A to D) Littermates at the age of 5 to 6 months were analyzed. Mean values ± standard deviations for 3 mice are shown for each panel.

Sperm maturation and motility are independent of PASKIN. Since functional antibodies derived against PASKIN are not available so far, we could not directly analyze subcellular PASKIN protein localization in spermatozoa and in mature sperm cells. However, the strong expression levels in postmeiotic stages of spermatogenesis suggest that PASKIN might have a function in sperm cells after leaving the testis. Therefore, sperm cells from caput epididymides, caudal epididymides, and vasa deferentia were isolated from wild-type, *Paskin*$^{+/-}$ and *Paskin*$^{-/-}$ mice and counted. As shown in Fig. 5A, the absence of PASKIN did not significantly affect sperm counts in these compartments. In addition, no difference in wet weight of any of these organs, including testis, relating to the *Paskin* genotype could be observed (data not shown). Sperm viability was also independent of the *Paskin* genotype (data not shown). CASA revealed no differences in the proportion of immotile, locally motile, and motile sperm cells isolated from caudal epididymides (Fig. 5B). Of the nonlinearly (Fig. 5C) and linearly (Fig. 5D) motile sperm cells, VCL, VAP, and VSL did not differ among wild-type and *Paskin* knockout mice. These data are consistent with the lack of difference in fertility in *Paskin* knockout mice (Table 1).

Coexpression of PASKIN and Sds22 during mouse spermatogenesis. Regarding the short promoter region shared by *Paskin* and *Ppp1r7*, coding for PASKIN and the protein phosphatase 1 subunit Sds22, respectively, we reasoned that Sds22 might be coexpressed together with PASKIN during mouse spermatogenesis. Sds22 mRNA could be detected by Northern blotting in all mouse organs analyzed, and the highest relative mRNA levels were found in the testis (Fig. 2). Like PASKIN mRNA, Sds22 mRNA expression increased during mouse puberty (Fig. 4C). As shown in Fig. 6A and B, two different polyclonal antibodies derived against Sds22 allowed the detection of Sds22 in various mouse organs, including the testis. As recently reported for the rat liver (27), multiple bands were detected with both antibodies in mouse liver, spleen, and kidney. However, in human and mouse testes, an Sds22 isoform of approximately 43 kDa was recognized by the N-terminal antibody (Fig. 6A) and an additional Sds22 isoform of approximately 45 kDa was primarily recognized by the C-terminal antibody (Fig. 6B and C). Sds22 protein expression in testis was independent of the *Paskin* genotype (Fig. 6C). Immunohistochemistry revealed an Sds22 expression pattern that resembled PASKIN expression, with a lack of expression in spermatogonia and detectable expression in spermatids and probably also spermatozoa (Fig. 6D).

DISCUSSION

The testis represents a unique environment where profound differentiation processes occur within a small compartment at

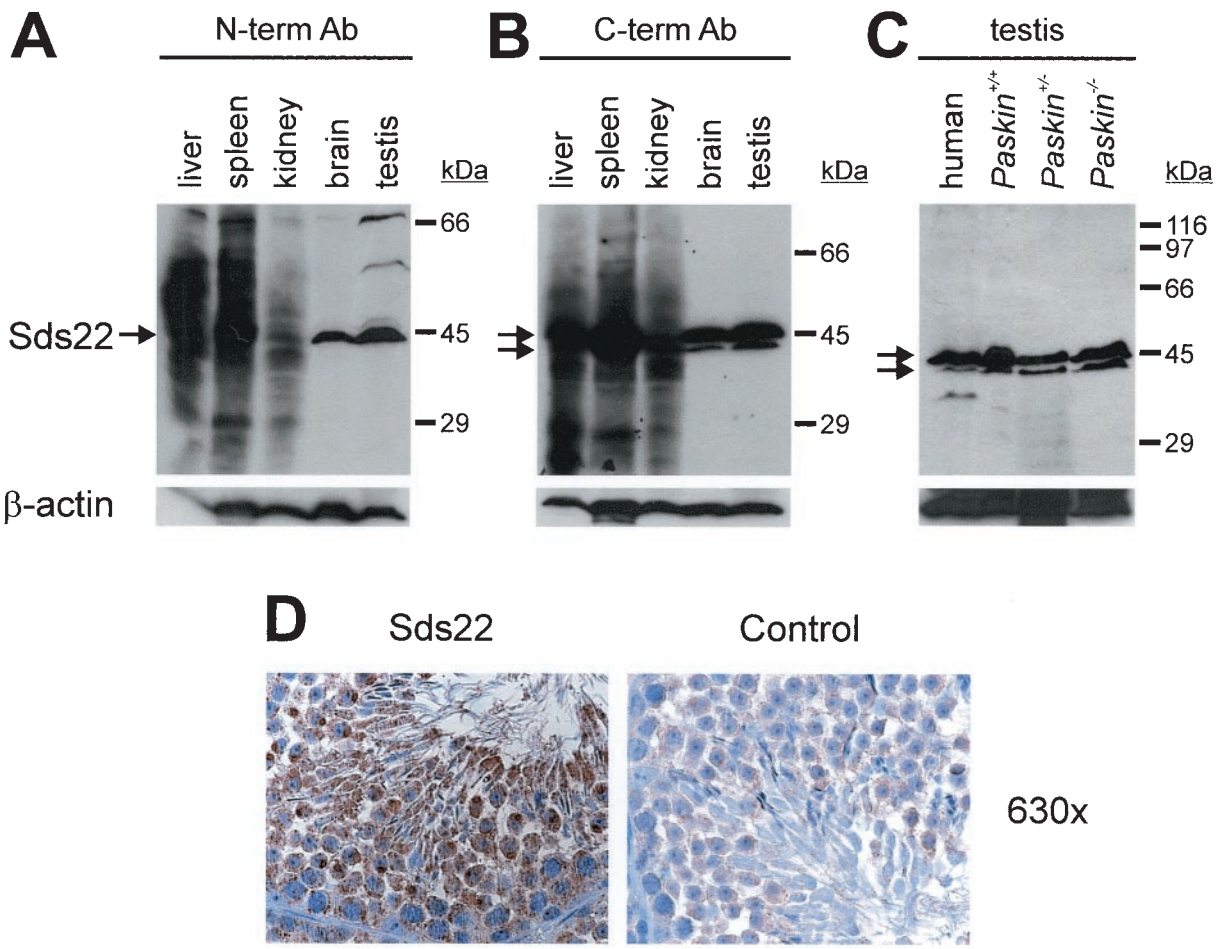

FIG. 6. Expression of the regulatory subunit 7 of protein phosphatase 1 (Sds22) in mice. (A to C) Immunoblot analysis of protein extracts derived from various wild-type mouse organs using polyclonal antibodies derived against N-terminal (A) or C-terminal (B) peptides of Sds22. (C) Immunoblot analysis of Sds22 protein expression in human and mouse testes derived from wild-type and *Paskin* knockout mice. (D) Indirect immunohistochemistry of testis cryosections with (Sds22) or without (control) an anti-Sds22 antibody. Original magnification, ×630. (C and D) The polyclonal antibody derived against the C terminus of Sds22 was used. Ab, antibody.

a high rate. Spermatogenesis is initiated by the differentiation of self-replicating spermatogonia at the basal layers of the seminiferous tubules to become committed intermediate spermatogonia. Following two further mitotic divisions, primary spermatocytes are formed which undergo the two rounds of meiotic divisions resulting first in secondary spermatocytes and then in haploid round spermatids. At this stage, chromatin is compacted and transcription is stopped. Specific mRNAs are stored for later translation of sperm-specific proteins. During mouse spermatogenesis, round spermatids mature in 16 distinct steps via elongated spermatids to mature spermatozoa. After about 13.5 days, spermatozoa are finally released into the lumen of the seminiferous tubules. Spermatogenesis appears in synchronized waves of layers of differentiating germ cells which sequentially migrate from the basal towards the luminal regions of the seminiferous tubules (21). Within this region, oxygen partial pressures as low as 2 mm Hg have been reported, which are among the lowest values found in the body and otherwise occur only in the vicinity of mitochondria (14). Regarding these developmental and environmental challenges, it is not surprising that a unique set of specific genes or splice variants of common genes are expressed exclusively in the testis. For example, testis-specific isoforms of glycolytic enzymes are expressed during the haploid stages of spermatogenesis and are still active in mature spermatozoa. In addition, we previously discovered a testis-specific isoform of hypoxia-inducible factor-1α, a master transcriptional regulator of oxygen-dependent glucose metabolism (13).

In the search for possible oxygen sensor proteins involved in regulating oxygen-dependent energy flux, we previously cloned PASKIN which combines in a single protein a FixL oxygen sensor-related PAS sensory domain and an AMP kinase-related serine/threonine kinase signaling domain (10). Rutter and colleagues showed that the yeast PASKIN orthologues PSK1 and PSK2 coordinately control translation and sugar flux under stress conditions in a (unknown) ligand-dependent manner (23). Thus, although probably not directly involved in oxygen sensing, the yeast data suggest a metabolic role for PASKIN in mammalian species. As shown in this work, targeted disruption of mouse *Paskin* did not result in any obvious phenotype. Aldolase mRNA expression, as a marker of glycolysis, was unaffected in most organs studied in *Paskin*$^{-/-}$ mice.

In the thymus, the organ with the second highest PASKIN mRNA levels, aldolase mRNA was increased in *Paskin*$^{-/-}$ mice. The significance of this finding is currently unknown, and further experiments are required to elucidate how PASKIN is involved in aldolase mRNA regulation in the thymus. However, mouse cryosections, including the thymus, stained with the periodic acid-Schiff reagent to roughly estimate tissue concentrations of glycogen and other carbohydrates revealed no differences in carbohydrate content related to the *Paskin* knockout (data not shown), indicative of no gross alterations in sugar flux.

PASKIN mRNA was known to be expressed in most mouse and human organs (10), and it was an unexpected finding that much higher levels of PASKIN are expressed in germ cells of mouse testis. Juvenile male *Paskin*$^{+/-}$ mice were analyzed during puberty to estimate the onset of induction of PASKIN gene expression. The different maturation stages of meiotic spermatocytes can be first distinguished between postnatal days 10 and 15, whereas postmeiotic spermatids do not occur before day 19 but are highly represented at days 22 to 24 (17). Our mRNA measurements of wild-type mice and the β-galactosidase staining data of *Paskin*$^{+/-}$ mice hence suggest that PASKIN expression is strongly upregulated in postmeiotic spermatids. However, regarding the in situ hybridization data of wild-type mice, we cannot exclude that PASKIN expression already begins during meiosis in spermatocytes, but this could not account for the strong increase in mRNA levels which correlates with β-galactosidase staining in postmeiotic spermatids.

Knowing that PASKIN is expressed at late stages of spermatogenesis, it would be interesting to determine its subcellular localization in spermatozoa. Unfortunately, functional anti-PASKIN antibodies could not be generated so far, and β-galactosidase reporter gene activity is only of limited significance, since protein half-life and localization might differ completely from the corresponding features of PASKIN. The first evidence for PASKIN localization (and function) in spermatozoa might come from data on Sds22, the gene product of *Ppp1r7* that shares the promoter region with the *Paskin* gene. Though the differences in expression levels were not as pronounced as for PASKIN, our data suggest that at least two Sds22 isoforms of approximately 43 and 45 kDa are coexpressed together with PASKIN in mouse testes. Chun et al. found a novel 55-kDa Sds22 splice variant in rat testes, termed Sds22α3 (5), and Huang et al. recently reported a 43-kDa Sds22 isoform in the principal piece of bovine sperm tails (11). Testis Sds22 associates with and regulates a testis-specific isoform of PP1, PP1γ2 (5, 11). Thus, it is tempting to speculate that testis-specific Sds22-PP1γ2 complexes target PASKIN in mature sperm cells.

At least under laboratory conditions, lack of PASKIN did not affect mouse sperm function or reproduction. Considering that yeast strains deficient for the PSK1 and PSK2 genes displayed a phenotype only at 39°C under nutrient-restricted conditions (23), mouse PASKIN might serve for the adaptation to environmental stress conditions. Initial motility experiments with isolated *Paskin*$^{+/+}$ and *Paskin*$^{-/-}$ sperm did not reveal any differences under conditions of nutrient starvation (data not shown). However, PASKIN might affect sperm maturation within the testis under stress conditions, the nature of which still remains to be discovered.

ACKNOWLEDGMENTS

This work was supported by the Deutsche Forschungsgemeinschaft (We2672/1-1 and Ka1269/5-1) and the Swiss National Science Foundation.

We thank A. Smith, M. Beullens, and M. Bollen for the gift of plasmids and antibodies and A.-K. Hellberg, S. Keller, C. Blatti, R. Landwehr, B. Saam, U. Lang, and G. Kersten for excellent technical assistance.

REFERENCES

1. **Amezcua, C. A., S. M. Harper, J. Rutter, and K. H. Gardner.** 2002. Structure and interactions of PAS kinase N-terminal PAS domain: model for intramolecular kinase regulation. Structure **10:**1349–1361.
2. **Bollen, M.** 2001. Combinatorial control of protein phosphatase-1. Trends Biochem. Sci. **26:**426–431.
3. **Ceulemans, H., A. Van Eynde, E. Perez-Callejón, M. Beullens, W. Stalmans, and M. Bollen.** 1999. Structure and splice products of the human gene encoding sds22, a putative mitotic regulator of protein phosphatase-1. Eur. J. Biochem. **262:**36–42.
4. **Ceulemans, H., V. Vulsteke, M. De Maeyer, K. Tatchell, W. Stalmans, and M. Bollen.** 2002. Binding of the concave surface of the Sds22 superhelix to the α4/α5/α6-triangle of protein phosphatase-1. J. Biol. Chem. **277:**47331–47337.
5. **Chun, Y. S., J. W. Park, G. T. Kim, H. Shima, M. Nagao, M. S. Kim, and M. H. Chung.** 2000. A sds22 homolog that is associated with the testis-specific serine/threonine protein phosphatase 1γ2 in rat testis. Biochem. Biophys. Res. Commun. **273:**972–976.
6. **Deng, C. X., A. Wynshaw-Boris, M. M. Shen, C. Daugherty, D. M. Ornitz, and P. Leder.** 1994. Murine FGFR-1 is required for early postimplantation growth and axial organization. Genes Dev. **8:**3045–3057.
7. **Dioum, E. M., J. Rutter, J. R. Tuckerman, G. Gonzalez, M. A. Gilles-Gonzalez, and S. L. McKnight.** 2002. NPAS2: a gas-responsive transcription factor. Science **298:**2385–2387.
8. **Gilles-Gonzalez, M. A., G. S. Ditta, and D. R. Helinski.** 1991. A haemoprotein with kinase activity encoded by the oxygen sensor of Rhizobium meliloti. Nature **350:**170–172.
9. **Gu, Y. Z., J. B. Hogenesch, and C. A. Bradfield.** 2000. The PAS superfamily: sensors of environmental and developmental signals. Annu. Rev. Pharmacol. Toxicol. **40:**519–561.
10. **Hofer, T., P. Spielmann, P. Stengel, B. Stier, D. M. Katschinski, I. Desbaillets, M. Gassmann, and R. H. Wenger.** 2001. Mammalian PASKIN, a PAS-serine/threonine kinase related to bacterial oxygen sensors. Biochem. Biophys. Res. Commun. **288:**757–764.
11. **Huang, Z., B. Khatra, M. Bollen, D. W. Carr, and S. Vijayaraghavan.** 2002. Sperm PP1γ2 is regulated by a homologue of the yeast protein phosphatase binding protein sds22. Biol. Reprod. **67:**1936–1942.
12. **Katschinski, D. M., L. Le, D. Heinrich, K. F. Wagner, T. Hofer, S. G. Schindler, and R. H. Wenger.** 2002. Heat induction of the unphosphorylated form of hypoxia-inducible factor-1α is dependent on heat shock protein-90 activity. J. Biol. Chem. **277:**9262–9267.
13. **Marti, H. H., D. M. Katschinski, K. F. Wagner, L. Schäffer, B. Stier, and R. H. Wenger.** 2002. Isoform-specific expression of hypoxia-inducible factor-1α during the late stages of mouse spermiogenesis. Mol. Endocrinol. **16:**234–243.
14. **Max, B.** 1992. This and that: hair pigments, the hypoxic basis of life and the Virgilian journey of the spermatozoon. Trends Pharmacol. Sci. **13:**272–276.
15. **Morais Cabral, J. H., A. Lee, S. L. Cohen, B. T. Chait, M. Li, and R. Mackinnon.** 1998. Crystal structure and functional analysis of the HERG potassium channel N terminus: a eukaryotic PAS domain. Cell **95:**649–655.
16. **Mountford, P., B. Zevnik, A. Duwel, J. Nichols, M. Li, C. Dani, M. Robertson, I. Chambers, and A. Smith.** 1994. Dicistronic targeting constructs: reporters and modifiers of mammalian gene expression. Proc. Natl. Acad. Sci. USA **91:**4303–4307.
17. **Nebel, B. R., A. P. Amarose, and E. M. Hackett.** 1961. Calendar of gametogenic development in the prepuberal male mouse. Science **134:**832–833.
18. **Ponting, C. P., and L. Aravind.** 1997. PAS: a multifunctional domain family comes to light. Curr. Biol. **7:**R674–R677.
19. **Reppert, S. M., and D. R. Weaver.** 2002. Coordination of circadian timing in mammals. Nature **418:**935–941.
20. **Rolfs, A., I. Kvietikova, M. Gassmann, and R. H. Wenger.** 1997. Oxygen-regulated transferrin expression is mediated by hypoxia-inducible factor-1. J. Biol. Chem. **272:**20055–20062.
21. **Russell, L. D., R. A. Ettlin, A. P. Sinha Hikim, and E. D. Clegg.** 1990. Histological and histopathological evaluation of the testis. Cache River Press, Clearwater, Fla.
22. **Rutter, J., C. H. Michnoff, S. M. Harper, K. H. Gardner, and S. L. Mc-**

Knight. 2001. PAS kinase: an evolutionarily conserved PAS domain-regulated serine/threonine kinase. Proc. Natl. Acad. Sci. USA **98:**8991–8996.
23. **Rutter, J., B. L. Probst, and S. L. McKnight.** 2002. Coordinate regulation of sugar flux and translation by PAS kinase. Cell **111:**17–28.
24. **Sambrook, J., E. F. Fritsch, and T. Maniatis.** 1989. Molecular cloning: a laboratory manual, 2nd ed. Cold Spring Harbor Laboratory, Cold Spring Harbor, N.Y.
25. **Schmidt, J. V., and C. A. Bradfield.** 1996. Ah receptor signaling pathways. Annu. Rev. Cell Dev. Biol. **12:**55–89.
26. **Taylor, B. L., and I. B. Zhulin.** 1999. PAS domains: internal sensors of oxygen, redox potential, and light. Microbiol. Mol. Biol. Rev. **63:**479–506.
27. **Tran, H. T., D. Bridges, A. Ulke, and G. B. Moorhead.** 2002. Detection of multiple splice variants of the nuclear protein phosphatase 1 regulator sds22 in rat liver nuclei. Biochem. Cell Biol. **80:**811–815.
28. **Wenger, R. H.** 2002. Cellular adaptation to hypoxia: O_2-sensing protein hydroxylases, hypoxia-inducible transcription factors, and O_2-regulated gene expression. FASEB J. **16:**1151–1162.
29. **Zhulin, I. B., and B. L. Taylor.** 1997. PAS domain S-boxes in archaea, bacteria and sensors for oxygen and redox. Trends Biochem. Sci. **22:**331–333.